Cloud Publications
International Journal of Advanced Remote Sensing and GIS
2015, Volume 4, Issue 1, pp. 1271-1285, Article ID Tech-454
ISSN 2320 - 0243

Cloud Publications

Research Article **Open Access**

Study of Reflectance Spectroscopy in River Sediments

Ismael L. Schneider[1], Elba C. Teixeira[1, 2], Silvia B.A. Rolim[1] and Bachir Hallouche[3]

[1]Programa de Pós-Graduação em Sensoriamento Remoto e Meteorologia, Universidade Federal do Rio Grande do Sul, Av. Bento Gonçalves, Porto Alegre, RS, Brazil
[2]Departamento de Pesquisa, Fundação Estadual de Proteção Ambiental Henrique Luis Roessler, Av. Borges de Medeiros, Porto Alegre, RS, Brazil
[3]Departamento de Química e Física, Universidade de Santa Cruz do Sul, Santa Cruz do Sul, RS, Brazil

Publication Date: 23 September 2015

Article Link: http://technical.cloud-journals.com/index.php/IJARSG/article/view/Tech-454

Abstract In the present study, Sinos River basin sediments of south Brazil were characterized using reflectance spectroscopy in 350-2500 nm range. This basin is located in an industrialized and densely populated area. The results focus on the influence of aluminum and iron content, particle size, organic matter, and mineral composition in the sediment samples. Fe and Al concentrations were determined by X-ray fluorescence. Clay minerals were determined by an X-ray diffractometer and reflectance spectral curves with a high-resolution spectroradiometer ASD Field Spec. Results of the mineralogical analyses showed that quartz, kaolinite, and smectite are scattered over the entire basin for most of the studied sites. Higher reflectance was observed for the samples after removal of the organic matter, indicating features associated with clay mineral and Fe. Likewise, higher reflectance was observed for the smaller size fraction, indicating the influence of mud in the spectral albedo. At the 2200 nm wavelength, the Al-OH bond of clay mineral was detected in the spectra. This was associated with Al content. Features due to the presence of iron oxides were observed between 470-580 nm and 650-850 nm.

Keywords *Clay Minerals; Reflectance Spectroscopy; Sediments; Sinos River*

1. Introduction

There is a great demand for rapid and predictive sediment data to be used in environmental monitoring (Cohen et al., 2005; Rossel et al., 2006). Reflectance spectroscopy is a useful technique for this type of analysis because it is a nondestructive, inexpensive and rapid method for characterizing different materials (Kemper and Sommer, 2002). One advantage of reflectance spectroscopy is that this technique can be used either in the field or in the laboratory. This technique also results in sample preservation and minimal reagent consumption (McCarty et al., 2002). Reflectance spectroscopy can be used to efficiently acquire data from a large number of samples. Additionally, a single spectrum can be used to evaluate different attributes of the sediment (McBratney et al., 2006; Alkimim et al., 2011).

Spectroscopy provides a high sensitivity to small changes in chemical composition and/or material structure. Variations in the material composition often cause changes in shape and position of the spectral absorption bands. Thus, because of the chemical variety usually present in these samples, spectral signatures can be quite complex and sometimes difficult to interpret (Clark, 1999). However, the increased knowledge of the natural variation in spectral characteristics and the causes of changes have increasingly allowed investigating with detail the chemical characteristics of the natural environment. The shape, intensity and absorption bands from the spectral curves enable determining the presence of certain constituents of the sediment, especially organic matter, clay minerals and Fe and Al oxides (Stoner and Baumgardner, 1981). Thus, spectroradiometry is considered a promising technique for sediment analysis.

The utility of multispectral remote sensing techniques for discriminating among materials is based on the differences that exist among their spectral properties. Because distinct spectral vibrations occur as a consequence of target conditions and environmental factors, intrinsic spectral features that appear in the form of bands and slopes in the visible and near infrared (350 to 2500 nm) bidirectional reflection spectra of minerals (and, consequently, rocks) are caused by a variety of electronic and vibrational processes. Among these processes, can be highlighted crystal field effects, charge-transfer, color centers, transitions to the conduction band, and overtone and combination tone vibrational transitions, which are discussed and illustrated with reference to specific minerals (Hunt, 1977). In general, each of these minerals has its “spectral signature” diagram which is obtained from spectral data collected from a large selection of minerals in order to summarize the optimum intrinsic information available from the spectra of particulate minerals. This diagram provides all references for the interpretation of visible and near infrared features that typically appear in remotely-sensed data. In this spectral region, the most commonly observed features in naturally occurring materials are due to the presence of iron in some form, or to the presence of water or OH groups.

Despite the advantages of reflectance spectroscopy, there are relatively few studies using this technique to characterize sediments (Malley and Williams, 1997; Moros et al., 2008; Moros et al., 2009). Therefore, as sediments act as contaminants reservoirs and provide a reasonably accurate history of river pollution (Filgueiras et al., 2002; Hang et al., 2009; Davutluoglu et al., 2011), it is clear that this is a useful tool for characterizing this important environmental matrix. In addition, providing a practical and economical way to characterize the sediments, this technique may help to understand how pollutants, e.g., metals behave in the environment.

In the present study, Sinos River basin sediments were characterized using reflectance spectroscopy in 350-2500 nm range. The influence of particle size, Fe, Al, and organic matter (OM) levels are discussed.

2. Area of Study

The Sinos River basin is located in the northeast of the state of Rio Grande do Sul, Brazil. The area covers 3,820 km^2 and crosses through 29 counties, of which 21 are within the Porto Alegre Metropolitan Area, the capital of the state (see Figure 1). The geographical boundaries are the Serra Geral the east, the Caí River basin to the west and north, and the Gravataí River basin to the south (Schneider et al., 2014). The Sinos River main course flow is 190 km, with the source at an altitude of 600 m and it discharges at an altitude of 12 m. Approximately 1.3 million people inhabit its basin (Schneider et al., 2014), representing 13% of the total population of the state concentrated in only 3.5% of its territory. The climate is subtropical with an annual average temperature of 20°C and about 1,600 mm of rain annually, well-distributed over the four seasons (FEPAM, 2006).

Schneider et al. (2014) describe that the Sinos River basin can be divided according to the corresponding section of the river into three different regions: upper, middle, and lower. In the upper section, characterized by a more rugged terrain and agricultural activities on small farms, were selected two sampling sites (Table 1). This 25 km section of the Sinos River shows high declivity, with altitudes ranging from 600 m to 60 m. One sample site was selected in the 125 km middle section of the basin (Table 1), approximately 125 km long, where the declivity of the Sinos River decreases. The Sinos River basin stretches are located in the Paraná basin volcano-sedimentary units (basalts from the Serra Geral Formation and sandstones from the Botucatu Formation) (Figure 2). In terms of geomorphological subdivision, the region is formed by the Campos Gerais Plateau, the Serra Geral, the Serra Geral Slopes and the Rio Grande do Sul Central Depression (Figure 3), and contains a major area of dense vegetation and small farms (Figure 4). However, as we approach the river mouth, one can see outcrops of recent alluvial deposits, of colluvial and alluvial deposits, and the Botucatu Formation (Figure 2), as well as an increase in population density and urbanization beyond industrial concentration (Figure 4). According to the State Environmental Protection Agency (FEPAM, 2006) the major sources of concern for the quality of the basin waters are the industrial activity (especially metallurgy, electroplating, steel mills, petrochemical industry, and tanneries), domestic sewages, and rice plantations. The lower Sinos River stretch consists of tributaries that drain large urban centers, especially the Luis Rau and Portão streams. Sampling sites for the lower section include points near the mouth of these streams and six additional sites along the main course of the Sinos River (Table 1). The point codes in Table 1 indicate the distance in kilometers from the sampling point to the mouth of the Sinos River.

Table 1: *Location of the Sediment Sampling Sites*

Site	Coordinates		Stretch of River
	X	Y	
SI 188	-50.263	-29.725	Upper
Rolante River	-50.470	-29.581	Upper
SI 096	-50.850	-29.686	Middle
SI 066	-51.046	-29.691	Lower
Luis Rau stream	-51.126	-29.734	Lower
SI 048	-51.126	-29.737	Lower
Portão stream	-51.195	-29.778	Lower
SI 036	-51.194	-29.779	Lower
SI 028	-51.191	-29.796	Lower
SI 019	-51.188	-29.838	Lower
SI 008	-51.238	-29.875	Lower

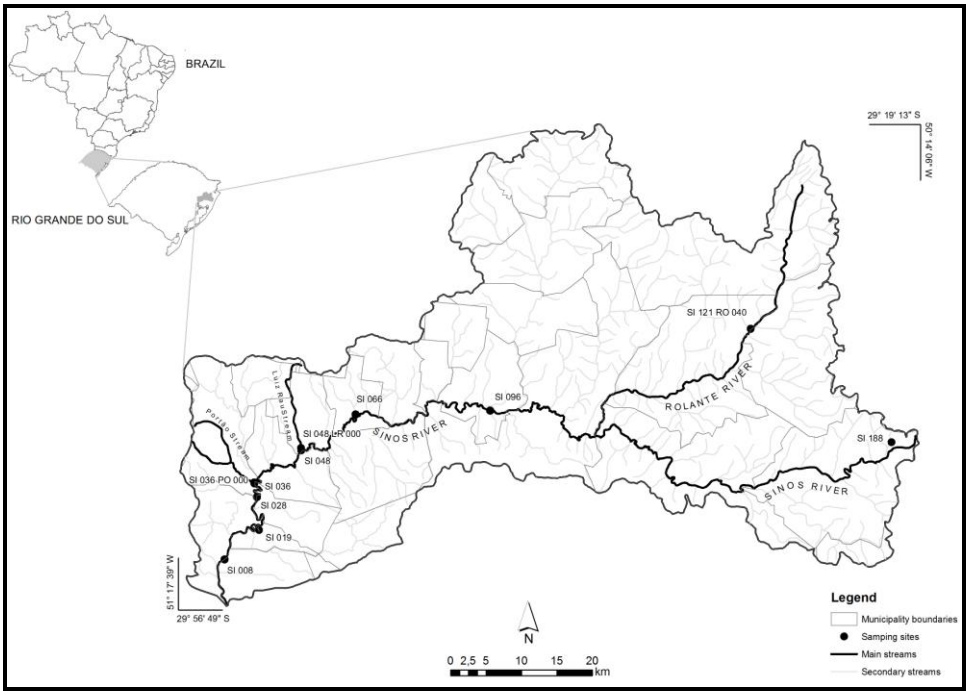

Figure 1: *Study Area with Location of Sampling Points*

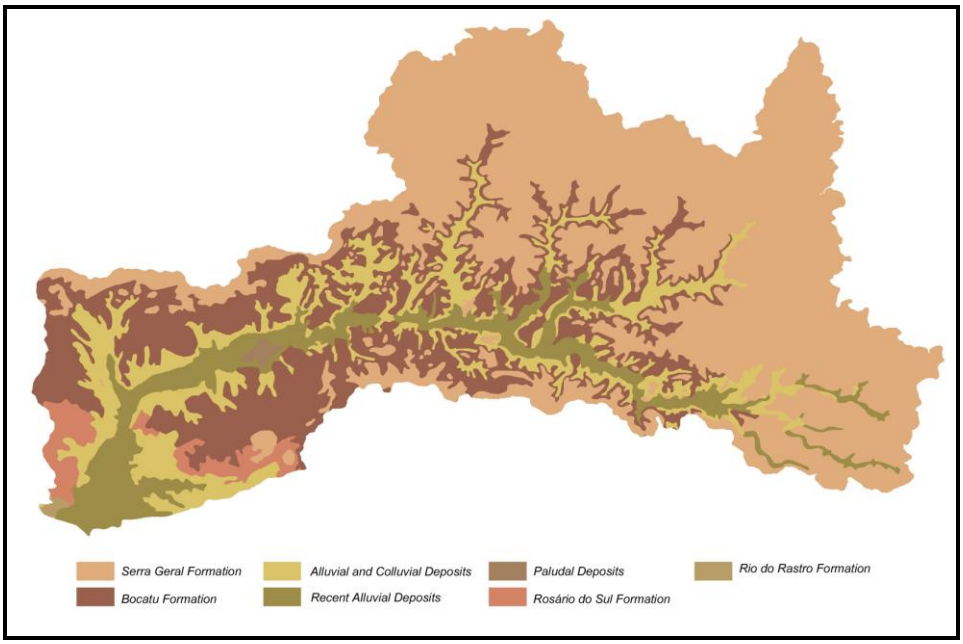

Figure 2: *Sinos River Basin Geological Map*

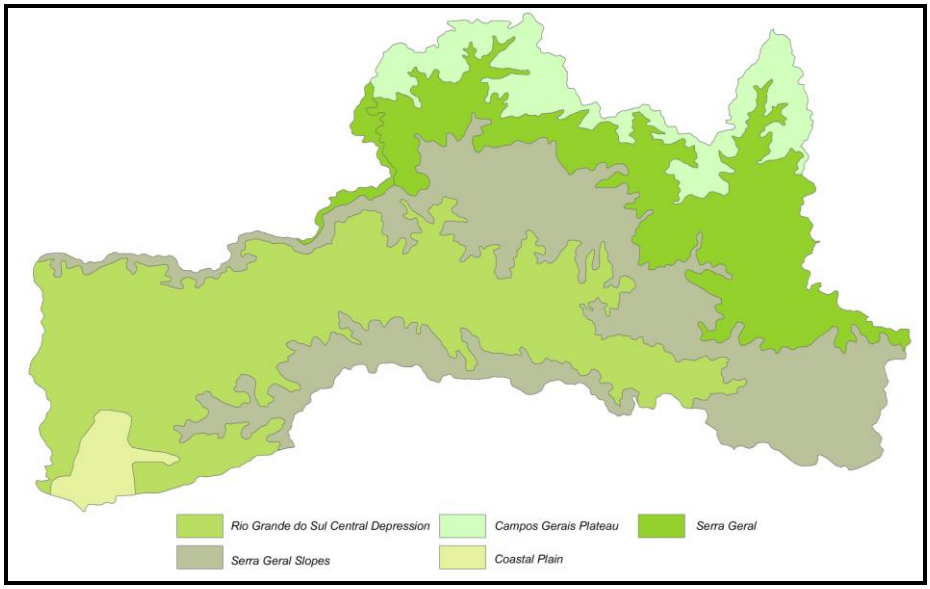

Figure 3: *Sinos River Basin Geomorphological Map*

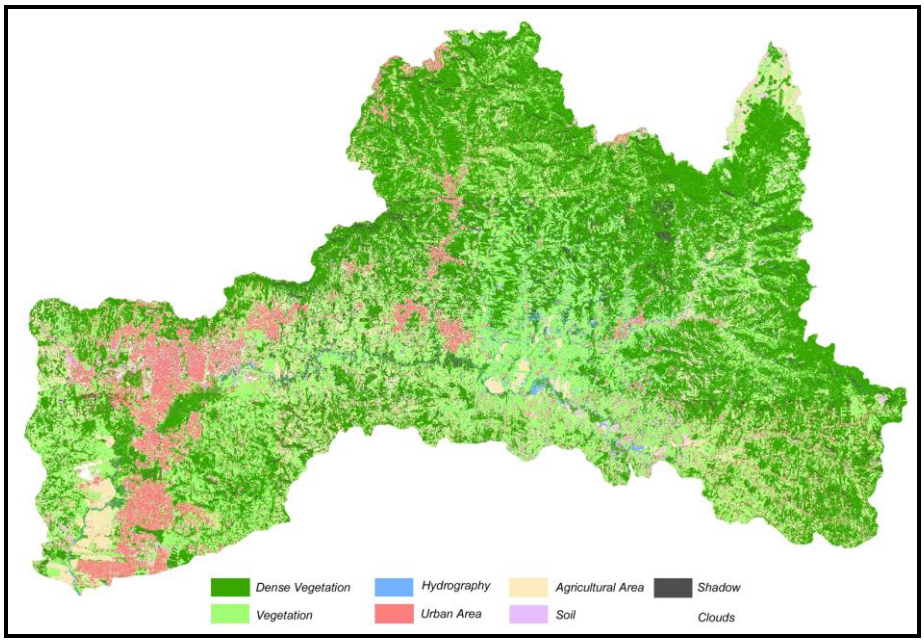

Figure 4: *Use and Occupation of Sinos River Basin from Supervised Classification in Rapid Eye Images*

3. Materials and Methods

3.1. Sampling

Eleven sediment samples were collected between February and August, 2010. They were selected eight points along the main course of the Sinos River and three tributaries (the Rolante River and the mouths of Luis Rau and Portão streams). Surface sediment samples were collected using a PVC L-shaped manual collector. The collected material was stored in plastic bags, cooled to 4 ºC, and sent to the laboratory, where a fraction of particle size <2 mm and another fraction of particle size <63 µm were separated via wet sieving. The organic matter was separated from the fraction with particle size <2 mm. The samples were oven-dried at 37 ºC and finely homogenized using an agate mortar. More information about sampling can be seen in the manuscript Schneider et al., (2014)

3.2. Determination of Particle Size Fractions, Clay Minerals, and OM, Fe and Al Contents

OM was obtained by the loss of mass by ignition (2 h at 360 °C) (Schulte and Hopkins, 1996). The analysis of particle size was performed in the laboratory of the Center for Coastal Studies (CECO) of the Federal University of Rio Grande do Sul. This technique involved the separation of the main textural classes of sediments by sieving and sedimentation. The clay minerals were analyzed after preparation of slides with the oriented clay minerals. The slides were air-dried, solvated with ethylene glycol and calcinated. The samples were then analyzed by an X-ray diffractometer between 2θ 2-28° using CuKα radiation (Rodrigues and Formoso, 2006; Schneider et al, 2014).

A procedure for the elimination of OM in the particle size fraction <2 mm with H_2O_2 was performed as described by Schneider et al. (2014).

To evaluate the sulphur (S), Fe and Al concentrations, the sediment samples were compressed into pellets and analyzed in a sequential X-ray fluorescence spectrometer (PW2404, Philips) equipped with a rhodium tube. The analysis was performed at the Analytical Geochemistry Laboratory at Campinas University.

3.3. Reflectance Spectroscopy

The objective of the spectral analysis was to analyze the interaction of electromagnetic radiation with the samples to identify the source material, as well as the influence of OM, iron oxides, mineralogy and grain size (Demattê et al., 2000; Alkimim et al., 2011). The sediment sample reflectance measurements in the laboratory were performed in particle fractions <2 mm, with and without OM, and <63 µm with a high-resolution spectroradiometer ASD FieldSpec®3 from Analytical Spectral Devices, Inc. (ASD). To identify the absorption features and minimize the effects of reflectance measurements, removal of organic matter in sediments was performed.

The reflectance equipment covers a spectral range between 350–2500 nm with a spectral resolution between 3–10 nm, interpolated at 1 nm. Lighting was provided by a halogen lamp positioned at an angle of 45° with the zenith, and a Spectralon calibration panel was used as a reference (100% reflectance). The geometry of the system was based on perpendicularly positioning the sensor in relation to the sample on a Petri dish at a distance of 5.6 cm between both. Four composite scans were obtained for each sample, with a 90º sample rotation between scans. The average of these scans was considered to describe the bidirectional diffuse reflectance of each sample (Ge et al., 2011).

Reflectance mode was used in this study because reflectance spectra of targets are immediately viewable allowing data quality to be monitored and immediate mineralogical analysis of the spectra to be carried out. Prior to each field measurement, reference spectra from a calibrated Spectralon™ tablet were collected in order to convert final measurements to absolute percent reflectance (Ferrier et al., 2009).

4. Results and Discussion

4.1. General Characteristics of the Samples

The samples were prepared in two particle sizes ranges (<63 µm and <2 mm). The spectra were acquired with the sediment in their entirety, dried and ground condition. In addition, spectra of the particles <2 mm were performed without OM to obtain a better interpretation of the absorption features (Figure 5).

In general, the sediments collected in the Sinos River have three well-defined spectral features correlated to the mineralogy of sedimentary and volcanic rocks of the Botucatu and Serra Geral Formations, even in the presence of organic matter. Strong absorption bands at 1400 nm and 1900 nm are due to the presence of water in the sediment compounds (Demattê et al., 1998; Meneses and Netto, 2001). An absorption band at 2200 nm is related to the presence of Al-OH vibration (Clark et al., 1990; Meneses and Netto, 2001; Chabrillat et al., 2002). The features due to iron, found between 450 and 600 nm (Hunt, 1977; Demattê et al., 1998; Meneses and Netto 2001), are subtle in the presence of OM, but become prominent after it is removed.

The mineralogical analyses showed that quartz, kaolinite, and smectite are scattered over the entire basin (Table 2). Kaolinite was not found at the Sinos River source (SI 188). According to Rodrigues and Formoso (2006), sediments containing smectite, which are expansive clays of high cationic exchange capacity, can retain metals. Thus, they are subject to remobilization due to changes in environmental conditions. Illite, zeolite, K-feldspar, and barite were also identified throughout the basin. These minerals were probably formed from alteration of volcanic rocks from the Serra Geral Formation and from sandstones of the Botucatu Formation (Oliveira et al., 2008). The same study also reports that at lower altitudes, corresponding to the lower Sinos River stretch, sediment deposition occurs due to the low water energy.

The total concentration of chemical elements in the sediments (fraction <63 µm, dry weight, with OM) of the Sinos River and its tributaries have high Cr concentration at the Portão stream (1,286 mg/kg) due to environmental markers of tannery effluents (Schneider et al., 2014). High concentrations of Cu, Ni, and Zn were also observed, especially in the Luis Rau stream sample, due to industrial activities. More details on the concentrations of chemical elements in the sediments can be found in the manuscript reported by Schneider et al. (2014).

Table 2 shows the results of characterizing sediment samples from the Sinos River basin. The highest S levels were found at the sites near the mouth of the Sinos River: SI 019, SI 008, and the Portão stream. These higher S levels may be attributed to the areas which are heavily influenced by chemicals used in the tannery and siderurgy industries. Similar behavior was reported by Rodrigues and Formoso (2006).

The higher content of OM was found at SI 188 and the Portão stream site (Table 2). The latter can be explained by the prevalence of industrial activities in the area. The former might be attributed to the influence of the well-preserved vegetation of the river margins and, derived from the decomposition of riparian vegetation leaves (Schneider et al., 2014).

Table 2: *Parameters used for Characterizing Sediment Samples from the Sinos River Basin*

Site	Particle Size Fraction (%)				Particle Size Classification	S (mg/kg)	OM (%)	Clay Minerals
	gravel	sand	silt	clay				
SI 188	75.0	16.2	7.7	1.0	gravel and sand	764	16.8	smectite, illite, quartz, zeolite
Rolante River	12.8	84.6	1.9	0.8	sand	394	10.6	kaolinite, smectite, illite, k-feldspar, quartz
SI 096	0.0	48.8	34.5	16.7	mud with sand	224	8.7	kaolinite, smectite, k-feldspar, quartz
SI 066	0.0	46.0	41.6	12.4	mud with sand	511	12.1	kaolinite, smectite, k-feldspar, quartz
Luis Rau stream	0.0	75.8	15.3	8.9	sand	267	11.1	kaolinite, smectite, illite, quartz
SI 048	0.0	71.3	19.5	9.2	sand with mud	286	10.0	kaolinite, smectite, k-feldspar, quartz
Portão stream	0.0	98.3	0.6	1.1	sand	922	15.8	barite, kaolinite smectite, quartz
SI 036	0.0	92.7	4.6	2.7	sand	637	9.8	kaolinite, smectite, illite, k-

								feldspar, quartz
SI 028	0.0	18.0	61.7	20.3	mud	729	11.5	kaolinite, smectite, quartz
SI 019	0.0	66.1	25.4	8.5	sand with mud	1301	12.0	kaolinite, smectite, k-feldspar, quartz
SI 008	0.0	52.2	37.4	10.3	sand with mud	1205	11.5	kaolinite, smectite, illite, quartz

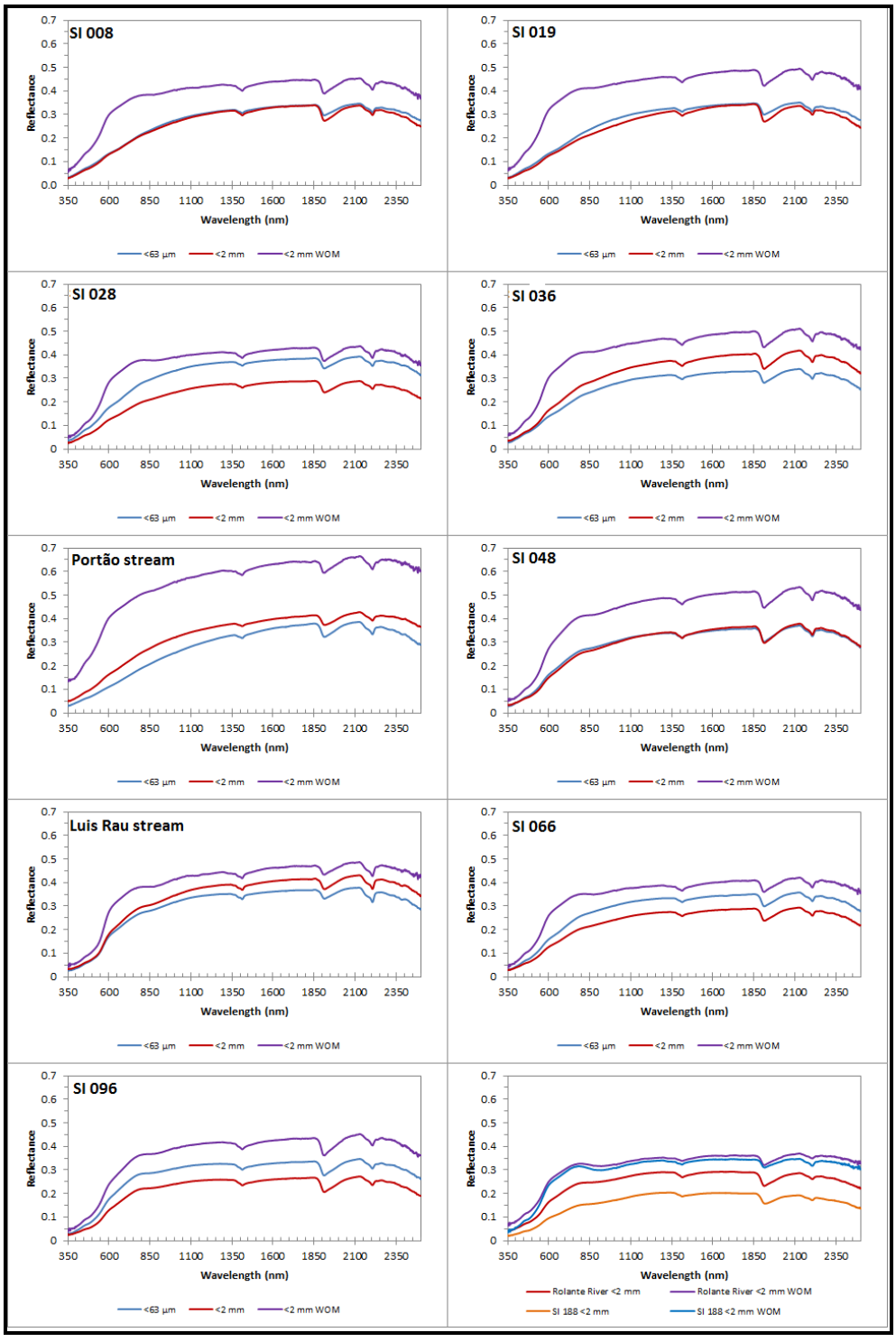

Figure 5: *Reflectance Spectra of Sediment Samples in 350-2500 Nm Range: Fractions <63 µm, <2 Mm with Organic Matter, and <2 Mm without Organic Matter - WOM*

4.2. Spectral Curve Analysis

Samples from the Upper Section (SI 188 and Rolante River)

These samples are from the source of the Sinos River, where there are few or no pollutants from industries. The sediment compounds are mostly sand (Rolante Stream and SI 188) and gravel (SI 188) from the Botucatu and Serra Geral Formations. These samples result in the lowest albedo for the spectral curves when compared to the middle and lower sections (Figure 5).

Sample from the Middle Section (SI 096)

This sample is still considered unpolluted due to receiving little or no anthropogenic contribution. The sediments in the sample were classified as mud with sand. The sample, with a reflectance up to 0.35 at 2130 nm, shows higher albedo for the <63 µm fraction spectral curves when compared to the upper section samples.

Samples from the Lower Section (SI 066, Luis Rau Stream, SI 048, Portão Stream, SI 036, SI 028, SI 019, SI 008)

These samples were near the source of the Sinos River, where industrial pollution such as siderurgy, metallurgy and tannery might have greatly influenced the results.

Classifications of sediments according to their particle size fraction are shown in Table 2. The fractions vary in concentration of gavel, sand, silt, and clay. This classification shows that there is mineralogical variability of sediments at the different sampling sites. However, the presence of organic matter could also potentially mask the spectral features (Demattê et al., 2000). As shown in Figure 5, the samples with a smaller particle size (i.e., those <63 µm) show higher reflectance than those with a particle size of 2 mm. This is because the smaller particles have a more uniform surface with fewer pores to retain incident light. Conversely, a larger particle size produces more irregular surfaces, which results in shading and a greater internal backscattering of the light. For the sediment samples <63 µm, the maximum reflectance ranged from 0.34 to 0.39 at 2126 nm (samples SI 028 and SI 036, respectively). Higher reflectance in SI 028 can be associated with the presence of mud in the particle size distribution (Table 2). Sample SI 036 showed the lowest reflectance, in the lower section, by presenting more than 90% sand in the particle size distribution.

Higher reflectance behavior for the fraction <63 µm, in relation to the fraction <2 mm for the samples without removal of OM, was not observed in the Portão stream, SI 036, and Luis Rau stream samples because these samples contained the highest percentages of sand. The samples SI 008, SI 019, and SI 048, classified as sand with mud, had similar reflectance to the fractions <63 µm and <2 mm with OM. The SI 096 and SI 066 samples exhibited higher reflectance in the <63 µm fraction than <2 mm with OM. This can be attributed to the sediment particle size classification, mud with sand, which favors higher reflectance due to the predominance of mud. Sample SI 028, classified as mud, also presented higher reflectance for the <63 µm fraction.

Figure 5 also displays the reflectance spectra for sediment samples in <2 mm fractions with and without OM. These results reveal an increase in the intensity of reflectance in samples without OM after chemical treatment (Demattê, 2002; Genú et al., 2010). There was found to be a reflectance increase for all sediment samples without OM (maximum values ranging from 0.35 to 0.66) when compared to samples with OM (maximum values ranging from 0.20 and 0.43).

Some authors reported that the decrease in reflectance concomitant with an increase in organic matter content occurs because the OM absorbs the energy, thereby decreasing the sample albedo (Demattê and Garcia, 1999; Demattê et al., 2000; Demattê, 2002; Genú et al., 2010). Furthermore, the presence of OM can mask the effect of the sediment's spectral response because OM absorbs energy, thereby decreasing the reflectance intensity (Fernandes et al., 2004; Genú et al., 2010).

When analyzing the reflectance spectra, all samples show an absorption band at 2200 nm (Figure 5), which is typical of the presence of kaolinite (Demattê, 2002; Fiorio, 2002; Genú et al., 2010). This is in agreement with the spectral curves in Figure 5 and the characterization of clay minerals in the sediment samples (Table 2). The spectral feature at 2200 nm may also be attributed to the Al-OH bond of clay minerals such as illite or smectite. In the sediment samples studied, the most important kaolinite effect was observed in the Luis Rau stream sample, due to their relationship with the higher concentration of Al (116 mg/g) and its characteristics (Tables 3 and 2). This sample showed the highest amplitude in the reflectance spectrum at 2200 nm, corresponding to 0.06 (Figure 7). In this figure, the samples without OM for most studied sites also show an intense feature at 2200 nm. This is not observed for the Rolante River and SI 188 samples. In the samples at these sites, the features of Al were less pronounced. This may be a result of the lower percentage of clays in these samples.

Table 3: *Total Al and Fe Concentrations in the Sediment Samples (fraction <63 µm, dry weight, with OM)*

Site	Al (mg/g)	Fe (mg/g)
SI 188	96.4	85.9
Rolante River	88.1	86.1
SI 096	96.9	81.2
SI 066	99.4	70.2
Luis Rau Stream	116	52.4
SI 048	98.0	68.9
Portão Stream	94.9	41.8
SI 036	100	63.8
SI 028	100	65.8
SI 019	96.7	62.4
SI 008	94.7	60.4

The remaining sediment samples showed Al concentrations between 88-100 mg/g. Their granulometric characteristics varied from sand to mud. In these samples, illite, kaolinite, and quartz were most probably formed by the alteration of rocks located near the source and the middle course of the Sinos River, including volcanic rocks of the Serra Geral Formation and sandstones beneath the Botucatú Formation (Oliveira et al., 2008). As mentioned previously, these authors also report that the lower Sinos River stretch corresponds to the low course of the river where the sediments are deposited due to low energy waters.

In Figure 6, the reflectance spectra for pure minerals show well defined Al-OH bonds at 2200 nm for the clay minerals found in the samples (kaolinite, illite and feldspar). The clay Al-OH bond shows absorption due to the presence of –OH groups, as was verified by some authors (Riazza, 1993; Demattê, 1995; Demattê et al., 1998). Thus, there is clearly a double feature at 2200 nm, in the curve of the pure mineral kaolinite (Figure 6), and less evident in sediment samples (Figure 5), due to the mineralogical variability of sediment in the sampling sites. This is important in the analysis of mineralogical composition and chemical analysis because this feature can be masked. The main spectral features of kaolinite are due to the hydroxyl (-OH) vibrations of its crystal lattice (Hunt, 1977).

Water peaks were present in all sediments samples analyzed at similar intensities in the reflectance spectra (Figure 5). This presence may be related to the similarity of water content in the samples, whose moisture content varied between 2.67-5.33%. The presence of water in these samples produced two absorption features in the reflectance spectrum, one at 1400 nm and other at 1900 nm. These bands are due to water molecule vibration of OH groups adsorbed on clay minerals (Hunt, 1980; Demattê et al., 1998; Meneses and Netto, 2001).

The iron oxides features were observed between 470-600 nm and a concavity at 850 nm was present in samples <2 mm without OM (Figure 5). The spectral curves with OM clearly show that the OM can mask the iron oxides features, as previously reported. However, the less prominent feature observed in the Portão stream sample may be related to the lower Fe level (Table 3). The features for Fe in the range of 470-600 nm have been reported by some authors (Demattê et al., 1998; Meneses and Netto, 2001; Genu et al., 2010). Others authors (Hunt, 1977; Vitorello and Galvão, 1996; Meneses and Netto, 2001) have indicated the presence of Fe in a concave shape in the spectral curve at 850 nm.

Table 3 presents the Fe levels, revealing higher values for samples taken from the Upper Section (SI 188 and Rolante River) and the Middle Section (SI 096) than samples from the Lower Section. This can be explained by the geology of the site, where elements are in the form of the hematite mineral-iron oxide III (Oliveira et al., 2008).

The feature at 450-550 nm is reported to be the presence of iron oxides (Genú et al., 2010). It has been described as goethite (FeOOH) and hematite (Fe_2O_3), the most frequent form of iron, Fe^{3+}, was found in sediment, resulting from the oxidation of iron, Fe^{2+}, present in the primary mineral during soil formation. Hematite and goethite are composed of Fe^{3+} in octahedral coordination with oxygen, however, goethite also has links of OH^- and hematite has links of O_2^- (Ben-Dor, 2002). The spectral features of iron result from electronic transitions of Fe^{3+}, however the iron oxides have different spectral responses at different wavelengths due to the structural differences of minerals. Some authors report absorption bands for Fe oxides in the range of 845-870 nm for hematite, and 900-930 nm and 650 nm for goethite (Genú et al., 2010).

Despite pure metals not absorbing energy in the visible and near-infrared region, these pollutants can be detected when they are complexed with organic matter, bound as hydroxides, sulfides, carbonates, or oxides. They can also be detected when they are adsorbed by clays that absorb light at this wavelength range (Hunt, 1977; Malley and Williams, 1997). However, when they are deposited in inorganic forms, the presence of metals can-not be detected by reflectance spectroscopy (Chodak et al., 2007). Some authors (Kemper and Somer, 2002; Moron and Cozzolino, 2003; Siebielec et al., 2004; Moros et al., 2008, 2009) have detected the metal concentrations in sediment samples. There was no detection of metals in the reflectance spectra of the sediment samples in this study. This may be due to the fact that these metals show their spectral features in the same wavelength regions of the Fe features, which is present at high concentrations in the samples, and Fe may be masking these characteristic absorptions.

Despite not having detected metals in the present study, some authors report features of Cu in sediments at 800 nm, Cr at 400 and 550 nm, Mn at 410, 450 and 500 nm, Ni at 400 and 740 nm, and Fe between 450-600 nm and 800 nm (Vitorello and Galvão, 1996; Demattê et al., 1998; Clark, 1999; Meneses and Netto, 2001).

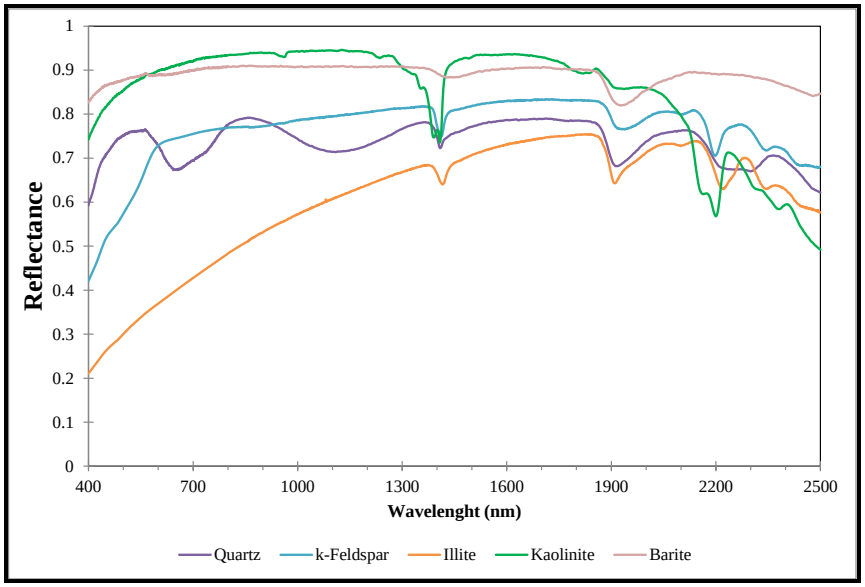

Figure 6: *Reflectance Spectra of Pure Mineral Obtained from the Spectral Library of NASA*

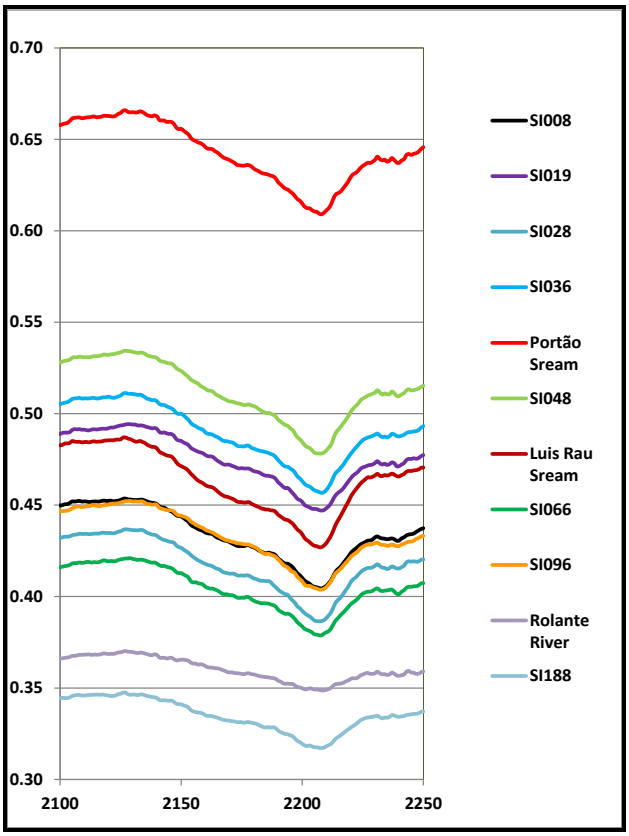

Figure 7: *Amplitude in the Reflectance Spectrum between 2100 and 2250 Nm*

5. Conclusions

This study revealed that reflectance spectroscopy can be used to characterize sediment and associate the spectral features with chemical and morphological characteristics. Characterization of sediments from the Sinos River basin by reflectance spectroscopy showed similar behavior across the sediment samples studied. The sediment samples without OM for the <2 mm fraction revealed higher

reflectance and reached maximum reflectance in the studied range. The Al-OH peak at 2200 nm was detected in the spectra and is associated with the presence of Al. This was most notable for the Luis Rau stream sample due to the higher concentration of Al at the sample site. The spectral curves for the <2 mm fraction without OM showed features of iron oxides between 470-580 nm and 650-850 nm. The Portão stream sample showed less prominent features at these wavelengths due to a lower Fe level. In the present study, only Fe and Al levels were observed in the spectral curves. High Fe levels in the samples might have masked detection of other trace metals. Grain size, organic matter, and mineral composition are factors that influence the features of absorption and reflectance intensity.

Acknowledgements

We are grateful to CAPES for financial support and to the Laboratory of Chemistry and Sampling Service of FEPAM.

References

Alkimim, A.F., Veloso, G.V., Lani, J.L., Gaspar, J., and Demattê, J.A.M. 2011: *Avaliação da reflectância espectral de solos representativos da bacia do rio Benevente com o emprego da análise de componentes principais.* Paper for the XV Simpósio Brasileiro de Sensoriamento Remoto (SBSR), 9064-9072, Curitiba, Brazil.

Ben-Dor, E. *Quantitative Remote Sensing of Soil Properties*. Advances in Agronomy. 2002. 75; 173-243.

Chabrillat, S., Goetz, A.F.H., Krosley, L., and Olsen, H.W. *Use of Hyperspectral Images in the Identification and Mapping of Expansive Clays Soils and the Role of Spatial Resolution*. Remote Sensing of Environment. 2002. 82 (2-3) 431-445.

Chodak, M., Niklinska, M., and Beese, F. *Near-Infrared Spectroscopy for Analysis of Chemical and Microbiological Properties of Forest Soil Organic Horizons in a Heavy-Metal-Polluted Area*. Biology and Fertility of Soils. 2007. 44 (1) 171-180.

Clark, R.N., 1999: *Spectroscopy of Rocks and Minerals, and Principles of Spectroscopy*. *Remote Sensing for the Earth Sciences: Manual of Remote Sensing*. John Wiley & Sons. 3-52.

Clark, R.N., King, T.V.V., Klejwa, M., and Swayze, G.A. *High Spectral Resolution Reflectance Spectroscopy of Minerals*. Journal of Geophysical Research. 1990. 95 (B8) 12653-23680.

Cohen, M.J., Prenger, J.P. and DeBusk, W.F. *Visible-Near Infrared Reflectance Spectroscopy for Rapid, Non-Destructive Assessment of Wetland Soil Quality*. Journal of Environmental Quality. 2005. 34 (4) 1422-1434.

Davutluoglu, O.I., Seckin, G., Ersu, C.B., Yilmaz, T. and Sari, B. *Heavy Metal Content and Distribution in Surface Sediments of the Seyhan River, Turkey*. Journal of Environmental Management. 2011. 92 (9) 2250-2259.

Demattê, J.A.M. *Characterization and Discrimination of Soils by their Electromagnetic Energy*. Pesquisa Agropecuária Brasileira. 2002. 37 (10) 1445-1458.

Demattê, J.A.M., Campos, R.C., and Alves, M.C. *Avaliação espectral de solos desenvolvidos em uma toposseqüência de diabásio e folhelho da região de Piracicaba, SP*. Pesquisa Agropecuária Brasileira. 2000. 35 (12) 2447-2460.

Demattê, J.A.M., and Garcia, G.J. *Alteration of Soil Properties through a Weathering Sequence as Evaluated by Spectral Reflectance*. Soil Science Society of America Journal. 1999. 63 (2) 337-342.

Demattê, J.A.M., Mafra, L., and Bernardes, F.F. *Comportamento espectral de materiais de solos e de estruturas biogênicas associadas*. Revista Brasileira de Ciência do Solo. 1998. 22 (4) 621-630.

Demattê, J.A.M., 1995: *Relações entre dados espectrais e características físicas, químicas e mineralógicas de solos desenvolvidos de rochas eruptivas*. PhD Thesis, Escola Superior de Agricultura Luiz de Queiroz, Universidade de São Paulo, 14.

FEPAM - Fundação Estadual de Proteção Ambiental. 2006. *Bacia Hidrográfica do Rio dos Sinos*. http://www.fepam.rs.gov.br/qualidade/qualidade_sinos/sinos.asp

Fernandes, R.B.A., Barrón, V., Torrent, J., and Fontes, M.P.F. *Quantificação de óxidos de ferro de latossolos brasileiros por espectroscopia de reflectância difusa*. Revista Brasileira de Ciência do Solo. 2004. 28 (2) 245-257.

Ferrier, G., Hudson-Edwards, K.A., and Pope, R.J. *Characterization of the Environmental Impact of the Rodalquilarmine, Spain by Ground-Based Reflectance Spectroscopy*. Journal of Geochemical Exploration. 2009. 100 (1) 11-19.

Filgueiras, A.V., Lavilla, I., and Bendicho, C. *Chemical Sequential Extraction for Metal Partitioning in Environmental Solid Samples*. Journal of Environmental Monitoring. 2002. 4 (6) 823-857.

Fiorio, P.R., 2002: *Dados radiométricos obtidos nos níveis terrestre e orbital na avaliação de solos.* PhD Thesis, Escola Superior de Agricultura Luiz de Queiroz, Universidade de São Paulo, 213.

Ge, Y., Morgan, C.L., Grunwald, S., David, J., Brown, D.J., and Sarkhot, D.V. *Comparison of Soil Reflectance Spectra and Calibration Models Obtained Using Multiple Spectrometers*. Geoderma. 2011. 161; 202-211.

Genú, A.M., Demattê, J.A.M., and Fiorio, P.R. *Spectral Analysis of Soils from Mogi-Guaçú (SP) Region*. Semina: Ciências Agrárias. 2010. 31 (1) 1235-1244.

Hang, X., Wang, H., Zhou, J., Du, C., and Chen, X. *Characteristics and Accumulation of Heavy Metals in Sediments Originated from an Electroplating Plant*. Journal of Hazardous Materials. 2009. 163 (2-3) 922-930.

Hunt, G.R., 1980: *Electromagnetic Radiation: The Communication Link in Remote Sensing*. John Wiley & Sons. 702.

Hunt, G.R. *Spectral Signatures or Particulate Minerals in the Visible and Near Infrared*. Geophysics. 1977. 42 (3) 501-513.

Kemper, T., and Sommer, S. *Estimate of Heavy Metal Contamination in Soils after a Mining Accident Using Reflectance Spectroscopy*. Environmental Science & Technology. 2002. 36 (12) 2742-2747.

Malley, D.F., and Williams, P.C. *Use of Near-Infrared Reflectance Spectroscopy in Prediction of Heavy Metals in Freshwater Sediment by their Association with Organic Matter*. Environmental Science & Technology. 1997. 31 (12) 3461-3467.

McBratney, A.B., Minasnya, M.L., and Rossel, R.V. *Spectral Soil Analysis and Inference Systems: A Powerful Combination for Solving the Soil Data Crisis*. Geoderma. 2006. 136 (1-2) 272-278.

McCarty, G.W., Reeves III, J.B., Reeves, V.B., Follett, R.F., and Kimble, J.M. *Mid-Infrared and Near-Infrared Diffuse Reflectance Spectroscopy for Soil Carbon Measurement*. Soil Science Society of America Journal. 2002. 66 (2) 640-646.

Meneses, P.R., and Netto, J.S.M., 2001: *Sensoriamento Remoto: reflectância dos alvos naturais*. UnB, Planaltina: Embrapa Cerrados. 262.

Moron, A., and Cozzolino, D. *Exploring the Use of Near Infrared Reflectance Spectroscopy to Study Physical Properties and Microelements in Soils*. Journal of Near Infrared Spectroscopy. 2003. 11 (1) 145-154.

Moros, J., Vallejuelo, S.F.O., Gredilla, A., Diego, A., Madariaga, J.M., Garrigues, S., and Guardia, M. *Use of Reflectance for Infrared Spectroscopy Monitoring the Metal Content of the Estuarine Sediments of the Nerbioi-Ibaizabal River (Metropolitan Bilbao, Bay Of Biscay, Basque Country)*. Environmental Science & Technology. 2009. 43 (24) 9314-9320.

Moros, J., Barciela-Alonso, M.C., Pazos-Capeáns, P., Bermejo-Barrera, P., Peña-Vázquez, E., Garrigues, S., and Guardia, M. *Characterization of Estuarine Sediments by Near Infrared Diffuse Reflectance Spectroscopy*. Analytica Chimica Acta. 2008. 624 (1) 113-127.

Oliveira, M.T.G., Rolim, S.B.A., Mello-Farias, P.C., Meneguzzi, A., and Lutckmeier, C. *Industrial Pollution of Environmental Compartments in the Sinos River Valley, RS, Brazil: Geochemical – Biogeochemical Characterization and Remote Sensing*. Water, Air, & Soil Pollution. 2008. 192 (1-4) 183-198.

Riazza, A. *Study of Reflectance of Pre-Cambrian Detritic Rocks For Structural Analysis in the Visible and Near Infrared*. International Journal of Remote Sensing. 1993. 14 (5) 927-942.

Rodrigues, M.L.K., and Formoso, M.L.L. *Geochemical Distribution of Selected Heavy Metals in Stream Sediments Affected by Tannery Activities*. Water, Air, & Soil Pollution. 2006. 169 (1-4) 167-184.

Rossel, R.A.V., Walvoort, D.J.J., McBratney, A.B, Janik, L.J., and Skjemstad, J.O. *Visible, Near Infrared, Mid Infrared or Combined Diffuse Reflectance Spectroscopy for Simultaneous Assessment of Various Soil Properties*. Geoderma. 2006. 131 (1-2) 59-75.

Schneider, I.L., Teixeira, E.C., Rodrigues, M.L.K., and Rolim, S.B.A. *Metal Content and Distribution in Surface Sediments in an Industrial Region*. Annals of the Brazilian Academy of Sciences. 2014. 86 (3) 1043-1061.

Schulte E.E., and Hopkins, B.G., 1996: *Estimation of Soil Organic Matter by Weight Loss-on-Ignition. Soil Organic Matter: Analysis and Interpretation.* Madison: Soil Science Society of America, 21-31.

Siebielec, G., McCarty, G.W., Stuczynski, T.I., and Reeves III, J.B. *Near- and Mid-Infrared Diffuse Reflectance Spectroscopy for Measuring Soil Metal Content*. Journal of Environmental Quality. 2004. 33 (6) 2056-2069.

Stoner, E.R., and Baumgardner, F. *Characteristic Variations in Reflectance of Surface Soils*. Soil Science Society of America Journal. 1981. 45 (6) 1161-1165.

Vitorello, I., and Galvão, L.S. *Spectral Properties of Geologic Materials in the 400 to 2500 Nm Range: Review for Applications to Mineral Exploration and Lithologic Mapping*. Photo Interpretation. 1996. 34 (2) 77-99.